On the Relationship Between Wear and Thermal Response in Sliding Systems

M. Amiri · M. M. Khonsari · S. Brahmeshwarkar

Abstract Experimental results reveal that the temperature rise of two contacting bodies in relative sliding motion is related to the wear rate. Experimental wear tests pertain to a ring-on-ring configuration for two sets of contacting materials: Bronze SAE 40 on Steel 4140 and 70-30 Brass on Steel 4140. Temperature variation within the contacting bodies during the tests is measured using a thermocouple. It is shown that the temperature of the interface can effectively characterize the steady-state wear. The results of the present approach are verified by calculating Archard's wear coefficient using the relationships derived in this paper and compared to published values in literature.

1 Introduction

Wear is progressive loss of material from the surface of a solid body due to mechanical contact and relative motion with a solid, liquid, or a gaseous counter body. The interacting bodies, the interface material, and the operating environment, along with the parameters of the mechanical contact contribute to the behavior of the tribosystem. Wear is not an intrinsic property but is a characteristic of the tribosystem. Its behavior depends on the material properties, the lubrication type, the configurational conformity of the contact and its types—sliding, rolling, impacting, etc.—and the load. Yet, by far, sliding contact wear is the

M. Amiri · M. M. Khonsari (✉) · S. Brahmeshwarkar
Department of Mechanical Engineering, Louisiana State University, 2508 Patrick Taylor Hall, Baton Rogue, LA 70803, USA
e-mail: Khonsari@me.lsu.edu

most common and it occurs in a wide spectrum of rotating machinery such as in mechanical seals, clutches, joints, gears, gaskets, and washers, etc. In the present work, we focus our attention to the dry sliding wear between flat metallic surfaces in unidirectional sliding motion under steady-state condition. A steady-state condition in sliding wear is the condition in which the rate of material removal is approximately constant and the mass of third body particles in the contact also remains constant [1].

Let us turn our attention now to the energetic consideration of the problem. Pressing two bodies together and setting the contact in motion is always accompanied by dissipation of energy. The interfacial friction is known to be the main factor that controls the input energy in a sliding system. The energy dissipates into the contacting bodies, giving rise to wear [2]. The friction and heat dissipation are, therefore, intimately related.

The question surrounding the underlying relationship between the energy dissipation and wear has recently gained considerable attention as researchers have begun to apply the energy approach as to characterize the wear behavior in tribological contacts [2–4]. A particularly interesting result is due to the work of Ramalho and Miranda [3], who showed that the energy dissipated in the contact is linearly correlated with the wear volume during sliding wear and that the results can be used to quantify the wear coefficient in Archard's equation. Archard's wear equation relates the wear volume (W) to the normal load (N), the sliding distance (S) and the inverse of hardness (H) through a proportionality constant (K), often referred to as the wear coefficient [5].

$$W = K\frac{SN}{H} = \left(\frac{K}{H}\right)SN = kSN, \tag{1}$$

where $k = K/H$ is specific wear rate. The Coulomb friction model establishes that friction is proportional to the normal

applied load, $F = \mu N$. Therefore, assuming a constant friction coefficient, a proportional relation can be established between the wear volume and the friction force as:

$$W \propto FS. \tag{2}$$

For unidirectional sliding, the second term of expression (2) represents the work done by the friction force. Therefore, from the energetic approach, the volume of wear is directly proportional to the energy dissipated by friction. Indeed, experimental results of Ramalho and Miranda [3] reveal that the rate of change in the wear volume is linearly related to the dissipated energy and that the slope of the line represents an estimation of the wear coefficient, $k = W/SN$.

It is generally accepted that the most of the work done against friction during the wear process converts into heat, which in turn, manifests itself as an increase in temperature of the interface [6–8]. In some applications the temperature rise is so significant that it affects the mechanical and metallurgical properties of sliding surfaces—e.g., as accompanied by formation of oxide layer(s) on the surface or even by melting [6]—and thus drastically changes the behavior of tribological systems [9–12]. Therefore, it is no surprise that prediction of the temperature distribution within the contacting bodies, and particularly near-surface temperatures in sliding systems, has captured the attention of many researchers [6, 8, 13, 14]. Specifically, the assessment of either the temperature rise at the interface or the temperature distribution within the contacting bodies has become the focus of many papers; see for example [15–19].

The present work introduces a simple and effective technique to quantitatively characterize the wear behavior of a dry sliding system by measuring the contact temperature. In particular, it is shown that the temperature rise is linearly correlated with the material loss and the slope of the linear relationship is a measure of wear coefficient, K. It is to be noted that the applicability of the present approach may be restricted to a certain range of loads and velocities within which the material composition does not experience large changes.

2 Experimental

2.1 Description of Apparatus and specimen

The testing apparatus is Lewis Research model LRI-1A tribometer capable of providing loads up to 890 N. The spindle is rotated using a synchronous motor. The speed of rotation ranges from 0 to 5,000 rpm. The machine is capable of running at constant speed or multiple speeds in a
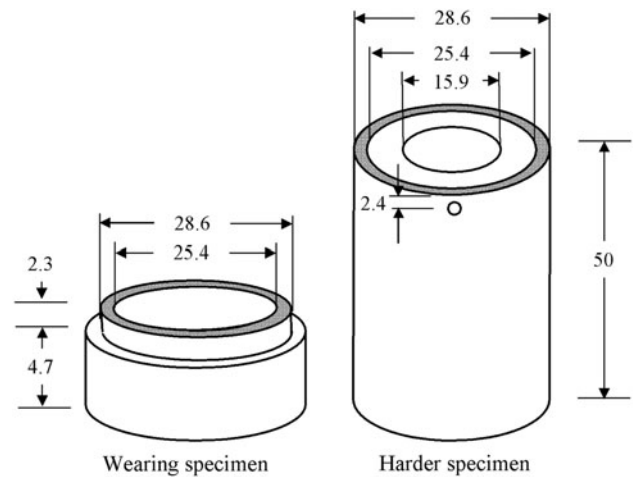
Fig. 1 Function pair (all dimensions are in mm)

single test. In this work, a thrust-washer type design for the wearing specimen and cylindrical shell type design for the harder material are used, providing a ring-on-ring contact configuration. The wearing material is affixed to the rotating spindle using a set screw. Figure 1 shows a drawing of the specimens used.

Figure 2 shows a schematic of the contact pair. The spindle does not move in the axial direction. The harder specimen is affixed in a socket of lower holder and is held stationary by an anti-rotating pin. The holder can move in the axial direction, that is, perpendicular to the sliding direction. The holder presses against the rotating part (fitted to the spindle) with a specified load. The automated loading arrangement ensures the application of the desired load
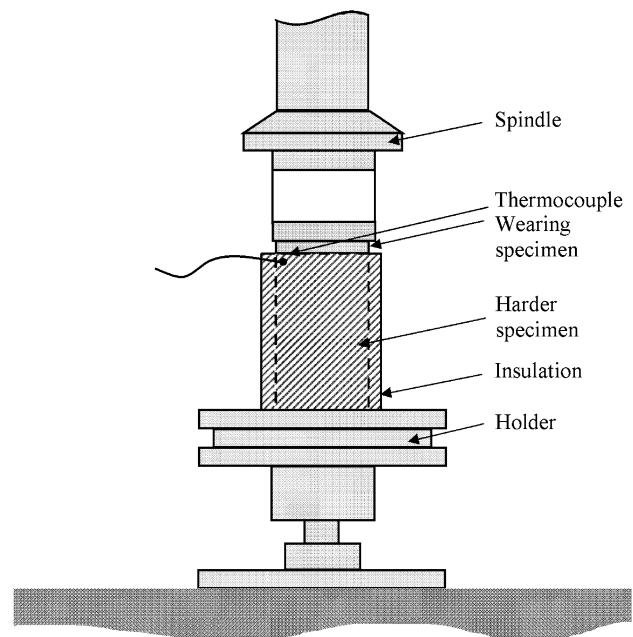

Fig. 2 Contact pair on the LRI-1a Tribometer

and maintaining it during the test. The contact is maintained throughout the test due to the constant axial push from the holder.

2.2 Wear Measurement

A linear variable differential transformer (LVDT) senses the displacement of the holder during the test, which is a measure of wear. The LVDT converts displacement in the axial direction into voltage. The computer connected to this machine is the user interface. Data from the LVDT can be viewed during the test. Note that the result displayed by the machine represents the total wear, i.e. the sum of the wear associated with each of the contacting materials. Also, the LVDT sensor cannot differentiate between thermal expansion and wear. When steady-state is reached, wear tends to increase linearly but the actual value of wear is more than the value obtained by the machine by an amount equal to the steady-state expansion of the contact bodies:

$$w_{\text{machine}} = w_{\text{actual}} - d_{\text{exp}}, \tag{3}$$

where d_{exp} is the steady-state expansion of the contacting bodies. In the present study, the wear rate is considered instead of actual wear. This way, d_{exp}, is a constant during steady temperature condition and has no effect on the analysis. The accuracy of the wear measurement of the tribometer is rated at 0.635 μm.

Experiments show that the softer copper-based specimens wear at higher rate than the hard Steel specimen. An experiment is conducted in which both specimens are weighed before and after testing. The result shows 15×10^{-4} gr mass removal for wearing specimen and only 3×10^{-4} gr for hard Steel specimen. This measurement verifies that wear of the softer material is significantly higher than that of the harder material.

2.3 Temperature and Friction Measurement

Temperature of the interface is a significant parameter during friction experiments. According to the guidelines prescribed by the manufacturer, the thermocouple placed in a hole bored on the curved surface of the cylindrical stationary specimen of diameter 1.6 mm as close as 2.4 mm from the interface, gives reasonable values that can be taken as representative of the interface temperature. The stationary specimen is insulated using an insulation foam tube wound around the specimen. The use of insulation eliminates the complications associated with the environmental effect on the temperature measurements. Temperature is recorded by Stanford Thermocouple Reader that records the values of the thermocouple connected to the stationary specimen. From instrumentation point of view, it is easier to install a thermocouple within the stationary hard

Steel than the rotating wearing specimen. Therefore, in the present study, the surface temperature measurement within the harder specimen is correlated with the wear rate of softer specimen. The tribometer is capable of measuring frictional force that is used to calculate the coefficient of friction.

2.4 Experimental Set-Up

Table 1 shows the contacting materials and their properties [20]. Nominal composition of Bronze specimen is 85% Cu, 5% Sn, 5% Pb, 5% Zn and that of Brass specimen is 70% Cu, 30% Zn. For each metal pair, four experiments are carried out that involve a combination of two loads and speeds as shown in Table 2.

The temperature and wear readings plotted for a typical test are shown in Fig. 3. Temperature value is recorded in the stationary specimen. In the test results shown in Fig. 3, after about 100 min the temperature reaches a steady-state. Note that during about first 10 min of the experiment, the LVDT records a negative displacement due to the thermal expansion of the contacting bodies. After the steady-state is reached, the thermal expansion is constant and the wear increases continuously. The wear data used for analysis are taken after the system reaches the steady-state condition. Referring to Eq. (1), increasing the normal load or sliding distance linearly increases wear. Increasing the normal load or sliding distance increases wear. However, the slope of the linear relationship depends on two parameters, i.e., the wear coefficient and the hardness, K/H.

Figure 4 shows the temperature rise in two tests. They pertain to subjecting the 70-30 Brass on Steel 4140 configuration to two different applied loads at a fixed sliding speed (0.282 m/s). Temperatures reported in Fig. 4 are measured at the location close to the interface. Referring to Fig. 4, a persistent trend emerges from both experiments. Initially, the temperature rises since the energy density associated with the friction work gives rise to generation of heat greater than the heat loss from the interface by conduction. Thereafter, temperature remains nearly constant, as the steady-state condition is reached (this occurs after about 100 min for the tests shown). As shown in Fig. 4, a greater applied load results in higher energy dissipation at interface and consequently higher temperature rise in the contacting bodies is experienced.

An idealization of the experimental temperature evolution is shown in Fig. 5. It reveals that the interface temperature increases during the first stage of the test, then remains almost constant (stage 2). The stabilization temperature in stage 2 or temperature gradient in stage 1 are directly proportional to the energy dissipation. The higher the energy dissipation, the greater the initial slope and the steady-state temperature becomes. Also shown in Fig. 5 is

Table 1 Contacting material properties

Wearing material	Thermal conductivity (W/m–K)	Specific heat const. pressure (J/kg-K)	Density (kg/m³)	Hardness (MPa)
SAE 40 Bronze	71.9	435	8.82×10^3	443.75
70-30 Brass	120	375	8.53×10^3	390.5
Steel 4140	42.7	500	7.85×10^3	2840

Table 2 Loading conditions for different metal pairs

Wearing material	Harder material	Load (N)	Speed (m/s)
SAE 40 Bronze	4140 Steel	17.79	0.141
SAE 40 Bronze	4140 Steel	17.79	0.282
SAE 40 Bronze	4140 Steel	13.34	0.141
SAE 40 Bronze	4140 Steel	13.34	0.282
70-30 Brass	4140 Steel	13.34	0.141
70-30 Brass	4140 Steel	13.34	0.282
70-30 Brass	4140 Steel	8.89	0.141
70-30 Brass	4140 Steel	8.89	0.282

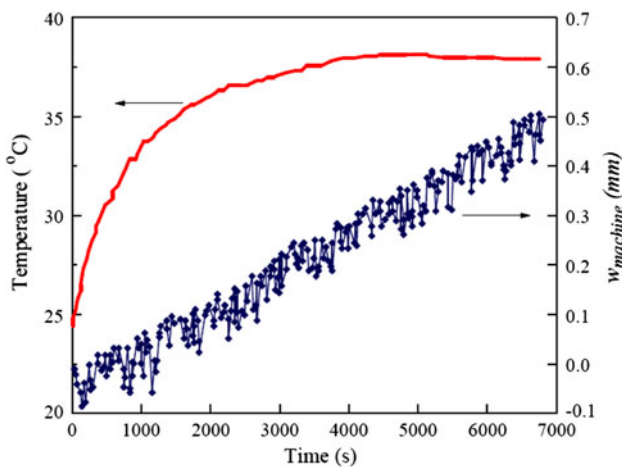**Fig. 4** Evolution of temperature rise for two tests at the location close to the interface

Fig. 3 Temperature data from thermocouple in the stationary specimen and wear data from LVDT for Bronze on Steel ($N = 17.79$ N, $S = 0.282$ m/s)
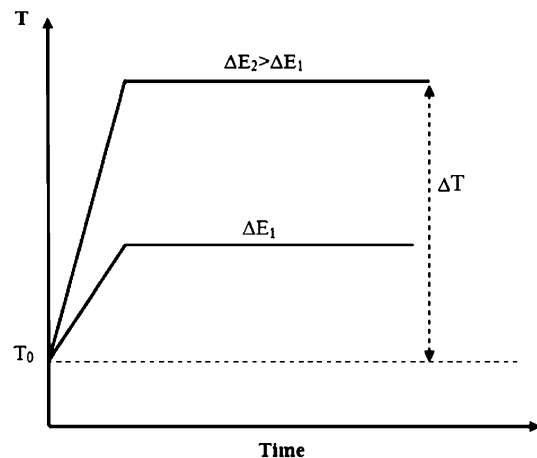
Fig. 5 Stabilized temperature increases as the energy dissipation increases

the temperature rise (ΔT) defined as the difference between the steady-state temperature and the temperature of the initial state (T_0). A higher temperature rise is associated with higher energy dissipation.

3 Results and Discussion

3.1 Experimental Results

Tables 3 and 4 show the measured wear rate, steady-state temperature and average of the coefficient of friction for all

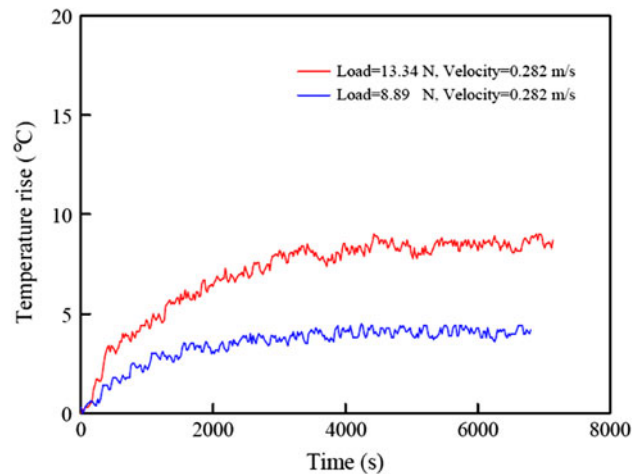the test conditions indicated in Table 2. Experimental results presented in this work are taken from Ref. [21].

The temperature rise during the sliding process is due to the frictional work. If the heat transfer to the surroundings is neglected, then all the dissipative heat generated during the sliding process is transferred into the sliding pair. In the present work, the use of insulation eliminates the heat transfer to surroundings. Neglecting the heat removed by

Table 3 SAE 40 Bronze on Steel 4140 test results

Sliding pair	Load (N)	Speed (m/s)	Steady-state temp. (°C)	Coeff. friction	Wear rate (μm/s) × 10³
Bronze–Steel (4140)	17.79	0.141	29	0.48	20.6
Bronze–Steel (4140)	17.79	0.282	38	0.33	51.3
Bronze–Steel (4140)	13.34	0.141	30	0.43	20.8
Bronze–Steel (4140)	13.34	0.282	35	0.51	41.3

Table 4 70-30 Brass on Steel 4140 test results

Sliding pair	Load (N)	Speed (m/s)	Steady-state temp. (°C)	Coeff. friction	Wear rate (μm/s) × 10³
Brass–Steel (4140)	13.34	0.282	32	0.46	75.1
Brass–Steel (4140)	13.34	0.141	30	0.55	41.7
Brass–Steel (4140)	8.89	0.141	29	0.56	34.5
Brass–Steel (4140)	8.89	0.282	30	0.49	53.4

the material loss due to wear, the net heat generation is divided between two bodies in contact. The division of the net heat between the contacting materials depends upon the relative thermal properties of the two sliding materials, and is characterized by the partitioning factor η. Figure 6 shows a schematic of two materials in contact as considered in the present study. Material 1 is moving with the sliding velocity of u while material 2 is stationary. Experimental temperature measurements are made within the stationary material (material 2).

Blok [22] and Jaeger [23] formulated the expression for the partitioning factor between two materials designated as 1 and 2. In the present configuration, assuming linear heat conduction, the following relationship for the heat partitioning factor can be obtained:

$$\eta_1 = \frac{\{C_{p2}k_2\rho_2\}^{\frac{1}{2}}}{\{C_{p2}k_2\rho_2\}^{\frac{1}{2}} + \{C_{p1}k_1\rho_1\}^{\frac{1}{2}}}, \qquad (4)$$

where C_{p1}, k_1, and ρ_1 are the specific heat capacity at
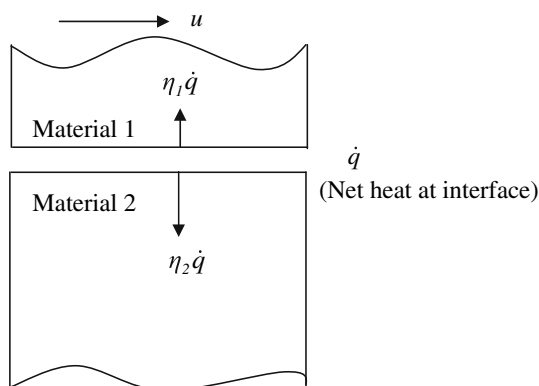

Fig. 6 Heat partitioning during sliding contact

constant pressure, thermal conductivity, and density of the material 1 and so on. Therefore, heat transferred to the material 1 is given by $\dot{q}_1 = \eta_1\dot{q}$ and the heat transferred to the material 2 is given by $\dot{q}_2 = \eta_2\dot{q}$, where $\eta_2 = 1 - \eta_1$. The heat generation transferred to the stationary specimen is then calculated as follows:

$$\dot{q}_2 = \eta_2\mu_{\text{ave}}uN \qquad (5)$$

where μ_{ave} is the average of coefficient of friction, N the normal applied load, and u the sliding velocity. It is assumed that in the present configuration the rotational speed has no significant effect on the partitioning factor. Figure 7 shows the measured wear rate against the heat transferred to material 2, $\dot{q}_2$. It reveals that the wear rate varies with the heat generation in approximately linear fashion, which confirms the discussion by Ramalho and Miranda [3]; that is, the energy dissipated in the contact is linearly correlated with wear. The goodness of the fit are $R^2 = 0.977$ in the case of Brass on Steel and 0.704 for Bronze on Steel, as indicated in Fig. 7.

Considering the relationship between wear rate and temperature, Fig. 8 shows the results of measured wear rate versus experimental steady-state temperature at the interface corresponding to those shown in Fig. 7. Note that linearity of variation between wear rate and temperature is much more prevalent with better goodness of the fit, particularly for the case of Bronze on Steel. Figure 8 reveals that wear rate is linearly dependent on the steady-state interface temperature and that the dependency is much more evident than the relationship between wear rate and heat dissipation as shown in Fig. 7. The strong relationship between wear rate and steady-state temperature at the interface offers a promising methodology for characterization of the tribological system.
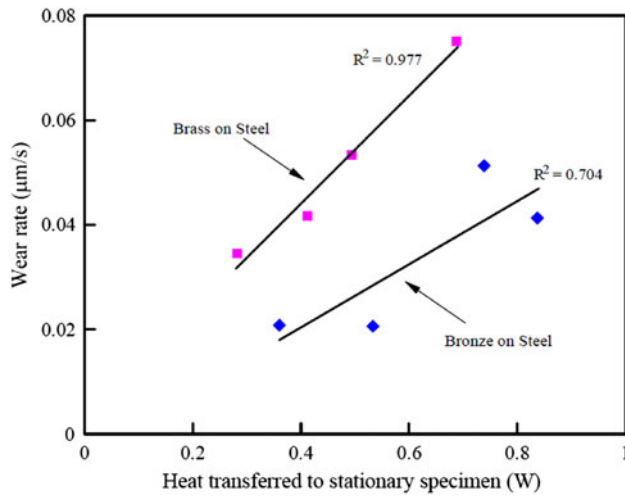
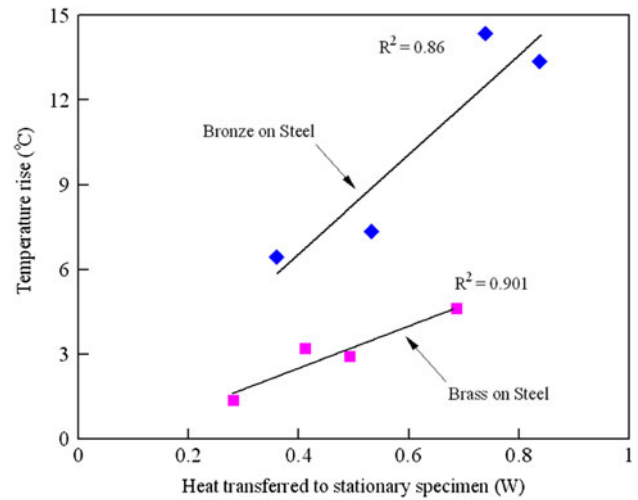**Fig. 7** Wear rate $\dot{w}$ against heat conducted to stationary specimen $\dot{q}_2$

Fig. 9 Steady-state temperature rise ΔT against heat conducted to stationary specimen $\dot{q}_2$

$$\Delta T = \Psi \dot{q}_2, \tag{6}$$

where Ψ is a constant. The experimental results presented in Sect. 3.1 show that the heat transferred to the stationary specimen, $\dot{q}_2$, is linearly related to wear rate, $\dot{w}$ (see Fig. 7 and the experimental work of Ramalho and Miranda [3]). A linear relationship between $\dot{w}$ and $\dot{q}_2$ can be assumed as:

$$\dot{w} = \xi \dot{q}_2, \tag{7}$$

where ξ is a constant. Eliminating $\dot{q}_2$ between Eqs. 6 and 7 yields:

$$\dot{w} = \xi \frac{\Delta T}{\Psi} = \frac{\xi}{\Psi} \Delta T. \tag{8}$$

Equation 8 establishes that wear has a linear relationship with temperature rise at interface during steady-state operation. It is to be noted that constant Ψ reflects the thermal behavior of contacting bodies in response to heat generation at the interface [24]. If the value of ξ is known, then one can easily predict the amount of wear by measuring temperature. Conversely, if data on wear and temperature are available, one can evaluate the constant ξ. We will refer to this constant as the wear index and establish a relationship between ξ and the wear coefficient K in Archard's classical wear law.

Elimination of normal load (N), between Eqs. 1 and 5 results in:

$$\dot{w} = \left(\frac{K}{\eta_2 \mu_{\mathrm{ave}} HA} \right) \dot{q}_2, \tag{9}$$

where A is the area of contact. In the aforementioned equation, it is assumed that the rate of change in wear volume, $\dot{W}$ is related to wear rate, $\dot{w}$ as $\dot{w} = \dot{W}/A$. Comparison of Eqs. 9 and 7 results in:
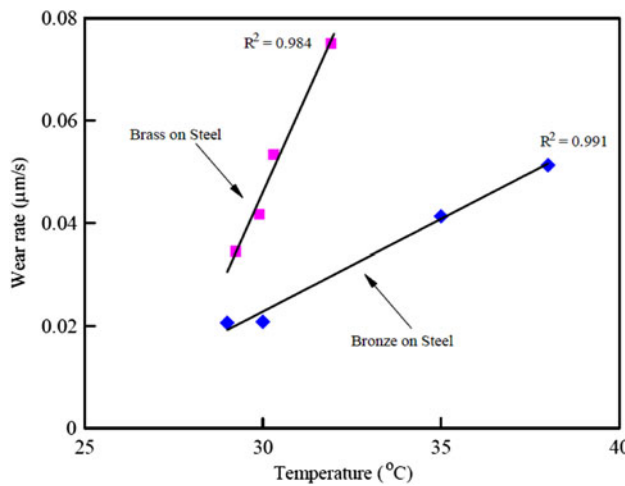

Fig. 8 Wear rate $\dot{w}$ against steady-state temperature near the interface for two tested materials

3.2 Evaluation of Wear Coefficient

Figure 9 shows the steady-state temperature rise of the stationary specimen at the location close (2.4 mm) to the interface plotted against the portion of the interfacial heat conducted to the stationary specimen. It can be seen that the relationship between the steady-state temperature rise and the heat transferred into the stationary specimen is approximately linear. The greater the heat generation at interface, the higher is the temperature rise during the steady-state condition.

The linearity between the temperature rise, ΔT during steady-state operation and the heat conducted to the stationary specimen, $\dot{q}_2$ can be formulated as follow:
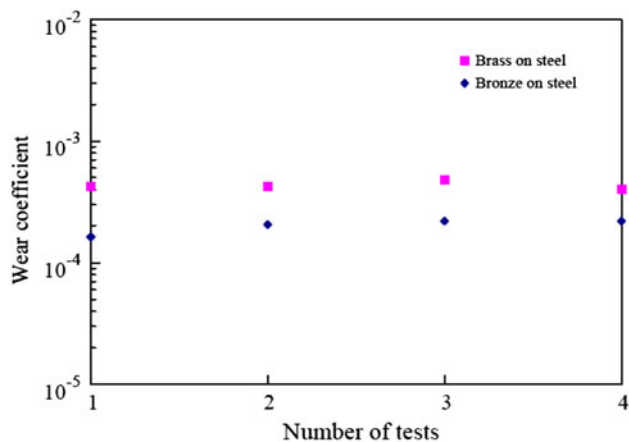
Fig. 10 Wear coefficient K for Bronze on Steel and Brass on Steel

$$\xi = \frac{K}{\eta_2 \mu_{\text{ave}} HA}. \tag{10}$$

Substitution of Eq. 10 into Eq. 8 gives a relation for the wear coefficient K as follows:

$$K = (\eta_2 \mu_{\text{ave}} HA\Psi)\frac{\dot{w}}{\Delta T}. \tag{11}$$

Equation 11 offers a methodology for evaluation of the wear coefficient based on the temperature measurements. If the interface temperature of the contacting materials is measured, one can evaluate the wear coefficient. It is worth noting that in the preceding analysis, the wear rate $\dot{w}$, comprised the wear of both soft and hard materials, thereby, the wear coefficient K, is obtained for pairs of contacting bodies. Figure 10 shows the calculated wear coefficients for Bronze and Brass on Steel for different operating conditions. The average value of wear coefficient obtained for the Brass on Steel pair is $K_{\text{Brass}} = 4.3 \times 10^{-4}$ and for Bronze on Steel pair is $K_{\text{Bronze}} = 2.02 \times 10^{-4}$. The published value of wear coefficient for Brass on Steel [25] and Bronze on Steel [26] are:

$$K_{\text{Brass}} = 6 \times 10^{-4}, \tag{12}$$

$$10^{-3} < K_{\text{Bronze}} < 10^{-4}. \tag{13}$$

Comparison of the wear coefficients obtained from the present method and those from work of Rothbart [25] and Rabinowicz [26] shows a very good agreement in the results.

With any experiment there is always a certain level of unavoidable uncertainty. An uncertainty analysis is performed (Appendix 1) to estimate the error associated with the calculation of wear coefficient. The performed error analysis merely takes into account the uncertainties of measuring devices, e.g., LVDT and temperature sensors. The calculations show that the maximum uncertainty for wear coefficient is ±7.3%. Considering the maximum

uncertainty of ±7.3%, the wear coefficient of Brass is $K_{\text{Brass}} = (4.3 \pm 0.314) \times 10^{-4}$. Similarly, with the maximum uncertainty of ±7.3%, the wear coefficient of Bronze is $K_{\text{Bronze}} = (2.02 \pm 0.147) \times 10^{-4}$. These values of wear coefficients are still in good agreement with Eqs. 12 and 13.

4 Conclusions

In the present work, an empirical approach of determining the wear coefficient based on the thermal response of a sliding system is presented. The approach involves relating the wear to interface temperature using experimental results. This relation is verified by considering a sliding contact in ring-on-ring configuration for two sets of contacting materials: Bronze SAE 40 on Steel 4140 and 70-30 Brass on Steel 4140. It is shown that the temperature of the interface can effectively characterize the behavior of the sliding system during steady-state wear conditions. Experimental results reveal that a higher temperature rise at the interface corresponds to higher energy dissipation and consequently higher wear rate. A linear relationship between the wear rate and the temperature rise at the steady-state condition is proposed. Applicability of the present method is limited to steady-state conditions for which no transitions in surface composition would be expected to occur. The verification, which involves comparison of the Archard's wear coefficient calculated using the present model with the published values, reveals a good agreement.

Appendix 1: Error Analysis

An uncertainty analysis performed using the method of Kline and McClintock [27]. This method uses the relative uncertainty in various primary experimental measurements to estimate the uncertainty of the final result. If the result of an experiment, R, assumed to be calculated from M independent parameters, $z_1, z_2, \ldots, z_M$ then the uncertainty propagated into the result, δR is:

$$\delta R = \sqrt{\sum_{i=1}^{M} \left(\frac{\partial R}{\partial z_i}\delta z_i\right)^2}, \tag{14}$$

where $\delta z_1, \delta z_2, \ldots, \delta z_M$ are the uncertainties of the independent parameters. Applying Eq. 14 to Eq. 11 gives:

$$\delta K = \sqrt{\left(\frac{\partial K}{\partial \dot{w}}\delta \dot{w}\right)^2 + \left(\frac{\partial K}{\partial(\Delta T)}\delta(\Delta T)\right)^2}. \tag{15}$$

It is to be noted that in the present error analysis, the uncertainties associated with wear rate, $\dot{w}$, and temperature,

T, measurements are only taken into account. The uncertainties associated with other parameters in Eq. 11 are neglected. The sensitivity coefficients in Eq. 15 can be obtained by differentiating Eq. 11 with respect to $\dot{w}$ and ΔT:

$$\frac{\delta K}{K} = \sqrt{\left(\frac{\delta \dot{w}}{\dot{w}}\right)^2 + \left(\frac{\delta(\Delta T)}{\Delta T}\right)^2}. \qquad (16)$$

A typical calculation for the test with $\dot{w} = 41.7 \times 10^{-3} \ \mu$m/s and $\Delta T = 3.2 \ ^\circ$C results in:

$$\frac{\delta K}{K} = \sqrt{0.06 \times 10^{-4} + 9.7 \times 10^{-4}} \approx \pm 3.1\%$$

uncertainty associated with the wear coefficient. The method of error analysis has been carried out for all the experimental data. The calculations show that the maximum uncertainty for wear coefficient is $\pm 7.3\%$.

References

1. Fillot, M., Iordanoff, I., Berthier, Y.: Wear modeling and third body concept. Wear **262**, 949–957 (2007)
2. Huq, M.Z., Celis, J.-P.: Expressing wear rate in sliding contacts based in dissipated energy. Wear **252**, 375–383 (2002)
3. Ramalho, A., Miranda, J.C.: The relationship between wear and dissipated energy in sliding systems. Wear **260**, 361–367 (2006)
4. Shakhvorostov, D., Pohlmann, K., Scherge, M.: An energetic approach to friction, wear and temperature. Wear **257**, 124–130 (2004)
5. Archard, J.F.: Contact and rubbing of flat surfaces. J. Appl. Phys. **24**, 981–988 (1953)
6. Wang, Y., Lei, T., Yan, M., Gao, C.: Frictional temperature field and its relationship to the transition of wear mechanisms of steel 52100. J. Phys. D Appl. Phys. **25**, A165–A169 (1992)
7. Dwivedi, D.K.: Sliding temperature and wear behavior of cast Al-Si base alloy. Mater. Sci. Technol. **19**, 1091–1096 (2003)
8. Li, W., Wang, Y., Yan, M.: Wear rate, frictional temperature, and energy consumption of steel 52100 with different microstructures during sliding. J. Mater. Sci. **40**, 5635–5640 (2005)
9. Lim, S.C., Ashby, M.F.: Overview no. 55 wear-mechanism maps. Acta Mater. **35**, 1–24 (1987)
10. Quinn, T.F.J.: Oxidational wear modelling: I. Wear **135**, 179–200 (1992)
11. Blau, P.J.: Friction and Wear Transitions of Materials: Break-In, Run-In, Wear-In. Noyes Publications, Park Ridge, NJ (1989)
12. Welsh, N.C.: Frictional heating and its influence on the wear of steel. J. Appl. Phys. **28**, 960–968 (1957)
13. Czichos, H.: Tribology: Systems Approach to the Science and Technology of Friction, Lubrication and Wear. Elsevier, Amsterdam (1992)
14. Kennedy Jr., F.E.: Thermal and thermomechanical effects in dry sliding. Wear **100**, 453–476 (1984)
15. Greenwood, J.A., Alliston-Greiner, A.F.: Surface temperature in a fretting contact. Wear **155**, 269–275 (1992)
16. Alyabev, Y.A., Kazimirchik, Yu.A., Onoprienko, V.P.: Determination of temperature in the zone of fretting corrosion. Mater. Sci. **6**, 284–286 (1973)
17. Bansal, D.G., Streator, J.L.: A method for obtaining the temperature distribution at the interface of sliding bodies. Wear **266**, 721–732 (2009)
18. Knothe, K., Liebelt, S.: Determination of temperatures for sliding contact with applications for wheel-rail systems. Wear **189**, 91–99 (1995)
19. Wen, J., Khonsari, M.M.: Transient temperature involving oscillatory heat source with application in fretting contact. ASME J. Tribol. **129**, 517–527 (2007)
20. ASM Handbook. Volume 2: Properties and Selection: Nonferrous Alloys and Special-Purpose Materials, 10th Edn. ASM International, Materials Park (1990)
21. Brahmeshwarkar, S.: A thermodynamic model for wear in sliding contact. M.Sc. dissertation, Louisiana State University, Baton Rouge (2006)
22. Blok, H.: Theoretical study of temperature rise at surfaces of actual contact under oiliness lubricating conditions. Inst. Mech. Eng. **2**, 222–235 (1937)
23. Jaeger, J.C.: Moving sources of heat and the temperature of sliding contacts. Proc. R. Soc. N. S. W. **76**, 203–224 (1942)
24. Ozisik, M.N.: Boundary Value Problems of Heat Conduction. Dover Publication Inc., New York (2002)
25. Rothbart, H.A.: Mechanical Design Handbook. McGraw-Hill, New York (1996)
26. Rabinowicz, E.: Wear Control Handbook. American Society of Mechanical Engineers, New York (1980)
27. Kline, S.J., McClintock, F.A.: Describing uncertainties in single-sample experiments. Mech. Eng. **75**, 3–8 (1953)